Chemical Engineering Journal 152 (2009) 492–497

Contents lists available at ScienceDirect

Chemical Engineering Journal

journal homepage: www.elsevier.com/locate/cej

Photocatalytic activities of Pd-loaded mesoporous TiO_2 thin films

Chih-Chieh Chan*, Chung-Chieh Chang, Wen-Chia Hsu, Shih-Kai Wang, Jerry Lin

Department of Chemical Engineering, Feng Chia University, No. 100 Wenhwa Road, Seatwen, Taichung 40724, Taiwan, ROC

ARTICLE INFO

Article history:
Received 31 January 2009
Received in revised form 28 April 2009
Accepted 8 May 2009

Keywords:
Photocatalytic
Mesoporous
TiO_2 thin film
Pd-loaded
Spin coating

ABSTRACT

In the present study, transparent nanocrystalline Pd–TiO_2 films were prepared by a sol–gel spin coating technique. By introducing non-ionic surfactant Triton X-100 into the sol, transparent mesoporous Pd–TiO_2 films were also prepared after calcination at 500 °C. To reveal the structural and morphological differences, the as-prepared TiO_2 and Pd–TiO_2 films were characterized by scanning electron microscope with energy dispersive spectrometer, thermal gravimetric analysis, X-ray diffraction and UV–vis spectrophotometer. In addition, the photocatalytic activities of these films were investigated by degrading methylene blue under UV and visible light irradiation. Sol–gel TiO_2 film, processed without surfactant, exhibited a pore-free smooth surface. Mesoporous TiO_2 and Pd–TiO_2 films with pore sizes ranging from 4 to 20 nm were obtained when surfactant was introduced and removed after calcination. In this study, the mesoporous Pd–TiO_2 film with molar ratio of Pd/Ti = 0.05 exhibited the best photocatalytic activity while specifically maintained good transparency.

1. Introduction

Crystalline TiO_2, especially anatase, has interesting properties and potential applications, e.g., photocatalysts [1], photoelectrodes [2], gas sensors [3], and electrochromic devices [4]. Anatase particles show a long catalytic lifetime, but for many applications, porous films with a large surface area are desired [5,6]. The photocatalytic activity of TiO_2 film depends strongly on the crystal structure, thickness, and porosity of the thin films. A highly porous structure is imperative among these factors because it offers a much larger number of catalytic sites than a dense structure. In addition, mesoporous materials are preferred over macroporous structures due to their higher active surface. Many papers have been published on the preparation of porous titania films using the sol–gel method [7], supercritical method [8], direct deposition from aqueous solutions [9], hydrothermal crystallization [10], ultrasonic spray pyrolysis [11], and sputtering technique [12]. Among these, the sol–gel process is one of the most appropriate technologies for the preparation of mesoporous thin oxide films, offering good homogeneity, ease of composition control, mild processing conditions, and large area coatings. Most reported examples of mesoporous TiO_2 materials prepared by the sol–gel process are limited to powdery forms. To obtain mesoporous TiO_2 thin films, it is important to strictly control the hydrolysis and condensation reactions of TiO_2 on the surface of organic templates forming a self-assembled phase in precursor solutions and to restrain the TiO_2 crystallization during calcination. It is technically crucial but very difficult to control the pore size, and at the same time, prepare thin film without yielding delaminating or cracking. Recently, surfactant or polymer templating techniques have been successfully applied in the sol–gel process to prepare mesoporous TiO_2 thin films. Among these structure-directing agents, polyethylene glycol (PEG) [13,14], polystyrene (PS) [15], and triblock copolymer (P123) [15] are the most frequently used polymer templates. Cationic CTAB, CTAC, and BTAC [16,17], anionic SDBS [17], and non-ionic Triton X-100 [18] are the most frequently used surfactant templates. Triblock copolymers are considered to be the potential structure-directing agents and to give the best mesoporous film structure, however, they are expensive and their synthesis is tedious. PEG is much cheaper, however, the resulting films have large pores and low porosity, as well as transparency and structure stability problems. Surfactant templates seem to be good compromises for addressing the significant trade-offs between cost and quality. In this study, we have successfully prepared transparent nanocrystalline and mesoporous TiO_2 thin films by a sol–gel spin coating technique with non-ionic surfactant Triton X-100 as a template.

There are two main obstacles for the practical application of TiO_2 photocatalyst: low quantum efficiency and restriction to short wavelength excitation. To solve these problems, several kinds of modification methods have been explored, such as noble metal doping [19,20], composite semiconductors [21–23], and transition or rare earth element doping [24–26]. The enhancement of quantum efficiency by the addition of noble metals may attribute to the rapid transfer of photogenerated electron from semiconductor to the noble metal particles, resulting in the effective separation of the electrons and holes [27]. In addition, they may extend TiO_2

* Corresponding author. Tel.: +886 4 24517250; fax: +886 4 24510890.
E-mail address: ccchan@fcu.edu.tw (C.-C. Chan).

1385-8947/$ – see front matter © 2009 Elsevier B.V. All rights reserved.
doi:10.1016/j.cej.2009.05.012

absorbance in the visible light region [28]. Several metals, especially Pt, Pd, Ag, Au, Cu, and Fe, have been used for doping within or over the surface of TiO_2 photocatalysts [29–36]. Most doped-TiO_2 photocatalysts studied were in powdery forms or nonporous thin films. Very few reports have been found for doped-TiO_2 mesoporous films [37]. It is believed that mesoporous TiO_2 thin films combined with noble metal loading will effectively enhance their photocatalytic activities. In this paper, a novel sol–gel method to prepare transparent Pd-loading TiO_2 thin films with nanocrystalline and mesoporous structure by surfactant templating is reported. The effects of addition of Pd and non-ionic surfactant Triton X-100 on the mesoporous structure and crystallinity of the films and their photocatalytic activities have been investigated. To the best of our knowledge, this is the first report showing the influences of Pd and Triton X-100 on the photocatalytic activities of transparent TiO_2 thin films with nanocrystalline and mesoporous structure. The photocatalytic activity of the obtained thin films was evaluated by the photocatalytic discoloration of methylene blue solution in the aqueous phase under UV and visible light irradiation.

2. Experimental

All chemicals were of reagent grade and used as received. TiO_2 and Pd–TiO_2 films were prepared via the sol–gel spin coating method. Precursor solutions for TiO_2 films were prepared by mixing titanium n-butoxide (1 mole, Acros Organics USA, grade: 99%) with anhydrous ethyl alcohol (15 mole, Showa Chem. Co., Japan, grade: 99.5%). De-ionized water (2 mole) was used for hydrolysis, and nitric acid (3 mole, Showa Chem. Co., Japan, grade: 70%) was added to the alkoxide solution as a catalyst. The solution was vigorously stirred for 24 h at room temperature before being used for spin coating. The resulting solution was stable for more than a week when stored under room temperature.

To prepare TiO_2 and Pd–TiO_2 mesoporous films, palladium chloride (0.05 mole, Acros Organics USA, grade: 59%Pd), cyclohexane (0.8 mole, Acros Organics USA, grade: ≥99%), and Triton X-100 (0.4 mole, Sigma–Aldrich Inc., USA, laboratory grade) were also used in addition to the alkoxide solution. $PdCl_2$ was used as the precursor for Pd loading, and Triton X-100 was used as a template for the preparation of mesoporous films. After mixing all compounds, the solution was vigorously stirred for 24 h at room temperature. The molar ratio of $Ti(OC_4H_9)_4$:C_2H_5OH:HNO_3:H_2O:C_6H_{12}:Trition X-100:$PdCl_2$ in the alkoxide solution was 1:15:3:2:0.8:0.4:x (x = 0.01, 0.03 and 0.05).

Silica glass plates (with a dimension of 5 × 5 cm) were used as the substrates. TiO_2 coatings were obtained by spin coating at 1000 rpm for 20 s. The process was repeated (without drying between each coating) up to five times. The as-spin-coated films were dried under room temperature for 15 min, heated at 80 °C for 1 h, and then calcined in air at 500 °C for 2 h. After drying, heating, and calcining procedures were performed, the organic materials and surfactant in the films were completely removed.

The morphology and EDS mapping of TiO_2 and Pd–TiO_2 films were observed using a field emission SEM with energy dispersive spectrometer (FESEM-EDS, HITACHI S4800, Japan). Thermal property was examined by TGA (Model 2950, TA Inst., USA). The heating rate was set at 10 °C/min in a temperature range of 30–700 °C. The TGA samples were made from both powders and films. The film samples were obtained by scratching the films on the as-spin-coated samples after 1 h of air-drying. The phase identification of samples was performed using XRD (MAC-MXP3, Japan) with Cu K_α radiation. The pore size was estimated by both SEM and BJH methods, and the specific surface area was determined by BET method (ASAP2020, Micromeritics, USA). Absorption spectra of the films were examined with a UV–vis spectrophotometer (Mini-D2T, Ocean Optics Inc., USA). Photocatalytic performances of the TiO_2 and Pd–TiO_2 films were evaluated by degrading methylene blue (2 ppm, 30 ml; Sigma–Aldrich Inc., USA, dye content: ≥82%) in a reactor (C-70G Chromato-Vue Cabinet, UVP Inc., USA) under UV (λ = 365 nm, 2.8 mW/cm^2) and visible light (C-70G white light, 0.4 mW/cm^2) irradiation. The distance between the light source and film sample was 10 cm. The concentration change of methylene blue, determined by the absorbance of the solution at 664 nm, was evaluated with a UV–vis spectrophotometer (HP 8452A, USA).

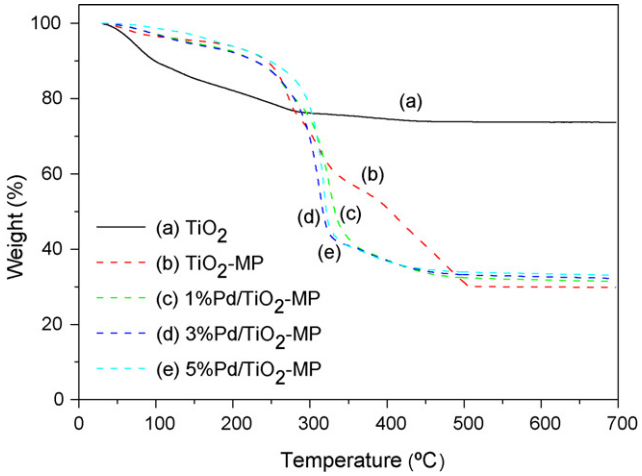

Fig. 1. TGA curves of TiO_2 and Pd–TiO_2 gel films.

3. Results and discussion

Thermal property of TiO_2 and Pd–TiO_2 gel films was investigated using TGA samples made from both powders and films. No significant difference between powder and film samples was found in the TGA results. In order to obtain highly mesoporous structure for TiO_2 and Pd–TiO_2 films, surfactant template has to be completely removed. In this study, non-ionic surfactant Triton X-100 was eliminated from the films by calcination method. Fig. 1 shows the TGA results of the heat-treated TiO_2 and Pd–TiO_2 films. The TiO_2 sample (sample a) displayed a three-step weight loss profile. The first weight loss below 100 °C was the removal of adsorbed water. The second weight loss ranging from 100 to 300 °C was attributed to the decomposition and combustion of organic compounds. The third weight loss ranging from 300 to 450 °C was due to the oxidation of residue carbon and the removal of structural hydroxyls, the combination of which increases the number of bridging oxygen and thus the monolithic nature of the gel matrix [38]. On the other hand, the Triton X-100-added TiO_2 samples exhibited apparently higher temperatures of the three regions than that of the single TiO_2 sample, which was attributed to its high molecular weight. For example, the temperature range of the three regions increased to 30–250 °C, 250–350 °C, and 350–500 °C, respectively. Among those mesoporous samples, TiO_2-MP (sample b) exhibited different weight loss process. The reason can be attributed to its smaller pore size than that of others (Fig. 2) and thus gives slower weight loss rate of surfactant residue, especially in the region from 350 to 500 °C. No further TGA weight loss was observed for samples calcined at/above 500 °C, indicating that surfactant and other organic substances in the samples can be completely decomposed and eliminated. This result was further proved in the following EDS mapping analysis. Thus, all films prepared in the following studies were calcined under 500 °C for 2 h.

The thickness of all films prepared in this study was estimated to be approximately 160 nm by SEM method. Fig. 2 shows SEM micrographs of heat-treated TiO_2 and Pd–TiO_2 films. No pores appeared

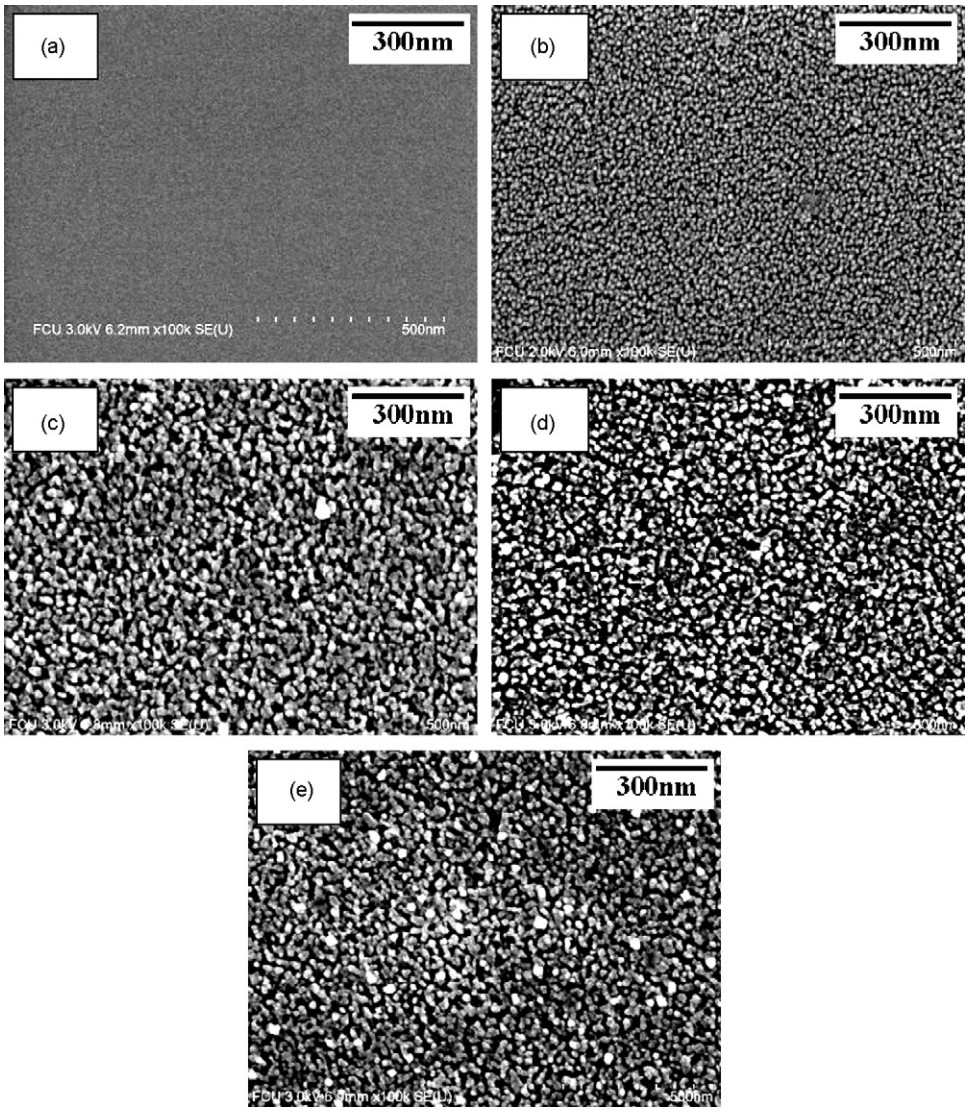

Fig. 2. SEM micrographs of films. (a) TiO_2, (b) TiO_2-MP, (c) 1%Pd/TiO_2-MP, (d) 3%Pd/TiO_2-MP and (e) 5%Pd/TiO_2-MP.

Table 1
Crystallite size, specific surface area and pore size of TiO_2 and Pd–TiO_2 films annealed at 500 °C.

Samples		XRD crystallite size (nm)	BET surface area (m^2/g)	Langmuir surface area (m^2/g)	Average pore diameter (4V/A by BET) (nm)	BJH adsorption average pore diameter (nm)	BJH desorption average pore diameter (nm)
(a)	TiO_2	6.0	9.72	16.03	3.47	2.27	1.11
(b)	TiO_2-MP	5.1	21.21	35.04	5.70	4.67	3.67
(c)	1%Pd/TiO_2-MP	5.8	39.93	65.33	5.15	4.45	3.78
(d)	3%Pd/TiO_2-MP	6.5	42.81	73.55	5.16	4.57	3.91
(e)	5%Pd/TiO_2-MP	6.7	44.05	72.06	5.15	4.58	3.92

Table 2
Element compositions of TiO_2 and Pd–TiO_2 films annealed at 500 °C.

Samples		Ti		O		Pd		Si	
		Weight%	Atom%	Weight%	Atom%	Weight%	Atom%	Weight%	Atom%
(a)	TiO_2	9.71	4.19	52.58	68.02	0	0	37.71	27.79
(b)	TiO_2-MP	8.55	3.72	50.76	66.10	0	0	40.69	30.18
(c)	1%Pd/TiO_2-MP	9.82	5.53	49.59	64.46	0.10	0.02	40.49	29.99
(d)	3%Pd/TiO_2-MP	10.44	4.82	49.25	65.01	0.69	0.14	39.62	30.03
(e)	5%Pd/TiO_2-MP	11.50	5.37	49.84	65.82	1.26	0.26	37.40	28.55

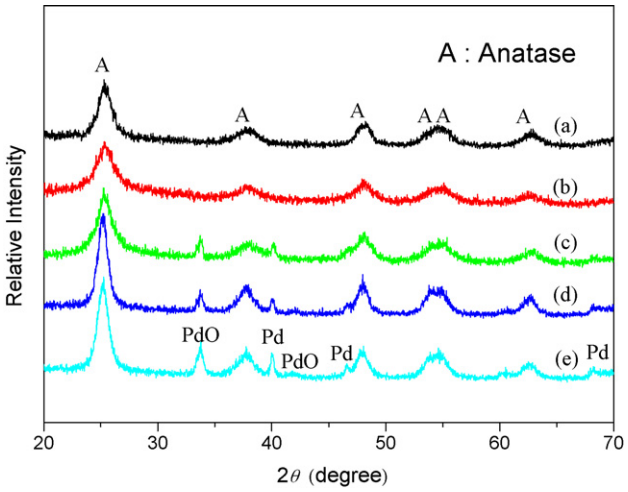

Fig. 3. XRD patterns of films. (a) TiO_2, (b) TiO_2-MP, (c) 1%Pd/TiO_2-MP, (d) 3%Pd/TiO_2-MP and (e) 5%Pd/TiO_2-MP.

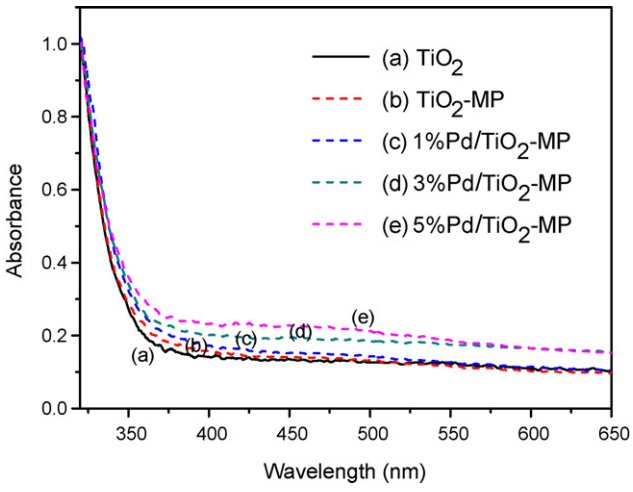

Fig. 4. UV–vis absorption spectra of TiO_2 and Pd–TiO_2 films.

in TiO_2 film prepared from the solution without surfactant Triton X-100. After Triton X-100 was added, mesoporous TiO_2 and Pd–TiO_2 films with pore sizes ranging from 4 to 20 nm were obtained. The formation of porous structure was attributed to the decomposition and elimination of surfactant in the gel films at 500 °C. As stated by Stathatos et al. [18], the presence of a non-ionic surfactant, Triton X-100, which bears a chain of approximately 10 ether groups, plays a crucial role in organizing the structure of material and in creating well-defined and reproducible nanophases. This family of surfactants participates in the formation and organization of clusters in solution, organizing the structure of the gel. Furthermore, shrinkage of the gels during drying is restricted by the incorporated surfactant micelles, which results in fine pore size and higher porosity of the calcined gels. Pores may also prevent the growth of TiO_2 crystals. Therefore, the presence of Triton X-100 decisively affects the structure of the films. SEM images (b)–(e) of Fig. 2 also show that the pore sizes of the films with Pd loading are larger than that without Pd addition. It is supposed that the self-organization ability of Triton X-100 in sol and its calcination behavior in gel are significantly influenced by the existence of Pd. The Pd dependence on the mesoporous structure of TiO_2 films has been corroborated by N_2 adsorption measurement as presented in Table 1. It can be observed that BET surface area of mesoporous TiO_2 films increased with increasing Pd content. The pore sizes estimated by BJH analyses range from 4 to 6 nm. Table 2 shows the EDS results of the film samples calcined at 500 °C. Ti, O, and Pd distributions in Pd–TiO_2 films are uniform and homogeneous (figure not shown). No C element was detected in the EDS mapping results of the samples; this is a further evidence of complete decomposition and elimination of surfactant and organic substances in the films.

Fig. 3 shows the XRD patterns of the 500 °C heat-treated TiO_2 and Pd–TiO_2 films. Six distinctive TiO_2 peaks can be found at 2θ of 25.3°, 37.8°, 48.0°, 53.9°, 55.1° and 62.7°, corresponding to anatase (1 0 1), (0 0 4), (2 0 0), (1 0 5), (2 1 1), and (2 0 4) crystal planes (JCPDF 21-1272), respectively, which indicate that the TiO_2 exists in the form of anatase phase after calcined at 500 °C. No observable rutile phase is observed in all samples. For Pd–TiO_2 films, three additional peaks can be obviously observed at 2θ = 40.1°, 46.7° and 68.1°, corresponding to (1 1 1), (2 0 0), and (2 2 0) crystal planes of metal Pd (JCPDF 89-4897), respectively, which not only further confirm the metallic state of the loaded palladium particles, but also shows their existed state as stable palladium crystals, which may promise improvement of catalyst performance. Since it is generally very easy to oxidize metal Pd into PdO phase in calcination environment under atmospheric air, two additional peaks at 2θ = 34.1° and 42.3° can also be observed, corresponding to (1 0 1) and (1 1 0) crystal planes of PdO (JCPDF 85-0713), respectively. Fig. 3 also shows the influences of Triton X-100 and Pd loading on the crystallinity of TiO_2 films. The Triton X-100-modified mesoporous TiO_2 film (sample b) has lower crystallinity than that of the nonporous single TiO_2 film (sample a). On the other hand, addition of Pd increases the crystallinity of the mesoporous TiO_2 films (samples c–e). It can be seen that an increase in Pd loading resulted in an intensity enhancement and narrowing of (1 0 1) peak, indicating a progressive growth of crystallites. The crystallite sizes of samples (a)–(e) are estimated to be 6.0, 5.1, 5.8, 6.5, and 6.7 nm, respectively, by using the Scherrer equation

$$d = \frac{k\lambda}{\beta \cos(\theta)} \quad (1)$$

where β (radians) is the full-width of half-maximum at 2θ of 25.3°, k is a constant (0.89), λ is the X-ray wavelength (1.541 Å for Cu K_α), d is the particle diameter and θ is the angle of the diffraction peak (degrees). It is supposed that the existence of pores in the films prevents the growth of TiO_2 crystallites while Pd loading enhances the coalescence of crystallites and their crystallinity.

The optical absorbance spectra of the prepared films were measured in the region of 300–800 nm and are shown in Fig. 4. It clearly exhibits the red shift of the absorption edge with increasing Pd content. It indicates the decrease of energy of excited photon owing to the presence of Pd. However, no significant difference of absorption edges was observed between nonporous TiO_2 film (sample a) and mesoporous TiO_2 film (sample b). The slightly difference of transmittance of samples (a)–(e) in the visible region (400–800 nm) may be due to the addition of Pd and the scattering of light by pores. It is believed that samples (a)–(e) have different sizes and numbers of pores.

The photocatalytic activities of TiO_2 and Pd–TiO_2 films are evaluated by degrading methylene blue under UV and visible light irradiation. Fig. 5 shows the typical time profiles of photodegradation of methylene blue under UV irradiation. As shown by the solid curve in Fig. 5a, pure poreless TiO_2 film shows only ~30% degradation of methylene blue after 6 h of UV illumination. Comparatively, mesoporous TiO_2 film increases the photocatalytic activity to ~80% degradation (Fig. 5b), being mainly attributed to the high active surface area. The high specific surface area increases the hydroxyl content of the films. In heterogeneous photocatalysis, the illumination of semiconductor produces electrons (e^-) and holes (h^+). The holes (h^+) combine with OH^- ions and there is formation of hydroxyl radicals ($h^+ + OH^- \rightarrow {}^\bullet OH$). These surface hydroxyl radi-

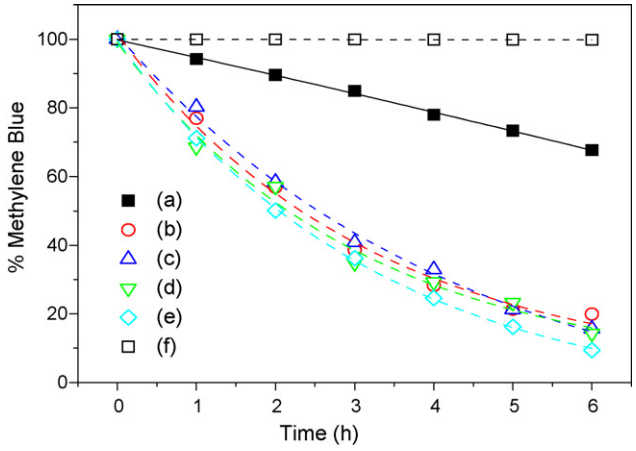

Fig. 5. Photodegradation curves of methylene blue under UV irradiation. (a) TiO_2, (b) TiO_2-MP, (c) 1%Pd/TiO_2-MP, (d) 3%Pd/TiO_2-MP, (e) 5%Pd/TiO_2-MP and (f) 5%Pd/TiO_2-MP-dark.

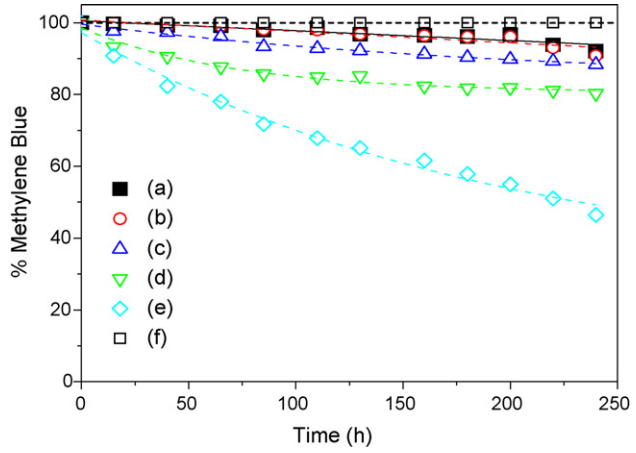

Fig. 6. Photodegradation curves of methylene blue under visible light irradiation. (a) TiO_2, (b) TiO_2-MP, (c) 1%Pd/TiO_2-MP, (d) 3%Pd/TiO_2-MP, (e) 5%Pd/TiO_2-MP and (f) 5%Pd/TiO_2-MP-dark.

cals formed on the surface of the photocatalyst are oxidizing species that ultimately enhance the photocatalytic activity [14]. Moreover, the addition of Pd further improves the photocatalytic activity of the mesoporous TiO_2 film. In this study, the mesoporous sample 5%Pd/TiO_2-MP exhibits the best photocatalytic performance; it decomposes 90% of methylene blue after 6 h of UV irradiation. The increase in photocatalytic activity with Pd loading is mainly attributed to the rapid transfer of photogenerated electron from semiconductor to the noble metal particles, resulting in the effective separation of the electrons and holes. This process of charge separation leads to an enhancement of the photoactivity, as the electrons can be trapped by adsorbed oxygen on the surface of the metal, and it may also account for the partial oxidation of palladium particles observed experimentally. In addition, the enhancement effect of Pd loading is also partly related to shift in optical absorption of the catalyst in visible region. This can be proved from the results of TiO_2 and Pd–TiO_2 films tested by the visible light excitation, which is shown in Fig. 6. It is apparently observed that only those samples with Pd loading exhibit significantly photocatalytic activity, which also increases with Pd content. A blank experiment resulted from a dark condition for sample 5%Pd/TiO_2-MP is also shown in Figs. 5 and 6. No concentration change of methylene blue was detected during the time courses.

4. Conclusions

In this paper, a novel sol–gel spin coating technique to prepare transparent Pd–TiO_2 thin films with nanocrystalline and mesoporous structure by surfactant templating is reported. The effects of addition of Pd and non-ionic surfactant Triton X-100 on the mesoporous structure and crystallinity of the films and their photocatalytic activities have been investigated. Nanocrystalline and mesoporous Pd–TiO_2 films with pore sizes ranging from 4 to 20 nm were obtained when surfactant was introduced during the preparation and removed after 500 °C calcination. UV–vis absorption spectra results show that the addition of Pd causes a small red shift change to the absorption edges of the mesoporous films. Nonporous TiO_2 film and mesoporous TiO_2 film were also prepared to compare with the mesoporous Pd–TiO_2 films. XRD shows that the Triton X-100-modified mesoporous TiO_2 film has smaller crystallite size and lower crystallinity than that of nonporous TiO_2 film, while the crystallite size and crystallinity of the mesoporous films increase with the Pd addition. In this study, the mesoporous Pd–TiO_2 film with molar ratio of Pd/Ti = 0.05 exhibits the best photocatalytic activity while specifically maintained good transparency.

References

[1] J. Yu, X. Zhao, Q. Zhao, Effect of surface structure on photocatalytic activity of TiO_2 thin films prepared by sol–gel method, Thin Solid Films 379 (2000) 7–14.
[2] S. Ito, T. Kitamura, Y. Wada, S. Yanagida, Facile fabrication of mesoporous TiO_2 electrodes for dye solar cells: chemical modification and repetitive coating, Sol. Energy Mater. Sol. Cells 76 (2003) 3–13.
[3] S.K. Hazra, S. Basu, High sensitivity and fast response hydrogen sensors based on electrochemically etched porous titania thin films, Sensor Actuators B Chem. 115 (2005) 403–411.
[4] C.S. Hsu, C.K. Lin, C.C. Chan, C.C. Chang, C.Y. Tsay, Preparation and characterization of nanocrystalline porous TiO_2/WO_3 composite thin films, Thin Solid Films 494 (2006) 228–233.
[5] B. Guo, Z. Liu, L. Hong, H. Jiang, Sol gel derived photocatalytic porous TiO_2 thin films, Surf. Coat. Technol. 198 (2005) 24–29.
[6] H. Yun, K. Miyazawa, I. Honma, H. Zhou, M. Kuwabara, Synthesis of semicrystallized mesoporous TiO_2 thin films using triblock copolymer templates, Mater. Sci. Eng. C 23 (2003) 487–494.
[7] J. Yu, X. Zhao, J. Du, W. Chen, Preparation, microstructure and photocatalytic activity of the porous TiO_2 anatase coating by sol–gel processing, J. Sol–Gel Sci. Technol. 17 (2000) 163–171.
[8] J.X. Jiao, Q. Xu, L. Li, T. Tsubasa, T. Kobayashi, Effect of PEG with different MW as template direction reagent on preparation of porous TiO_2/SiO_2 with assistance of supercritical CO_2, Colloid Polym. Sci. 286 (2008) 1485–1491.
[9] K. Shimizu, H. Imai, H. Hirashima, K. Tsukuma, Low-temperature synthesis of anatase thin films on glass and organic substrates by direct deposition from aqueous solutions, Thin Solid Films 351 (1999) 220–224.
[10] D. Zhang, T. Yoshida, H. Minoura, Low-temperature fabrication of efficient porous titania photoelectrodes by hydrothermal crystallization at the solid/gas interface, Adv. Mater. 15 (2003) 814–817.
[11] M.D. Blesic, Z.V. Saponjic, J.M. Nedeljkovic, D.P. Uskokovic, TiO_2 films prepared by ultrasonic spray pyrolysis of nanosize precursor, Mater. Lett. 54 (2002) 298–302.
[12] M.R. Teresa Viseu, M.I.C. Ferreira, Morphological characterization of TiO_2 thin films, Vacuum 52 (1999) 115–120.
[13] S.J. Bu, Z.G. Jin, X.X. Liu, L.R. Yang, Z.J. Cheng, Synthesis of TiO_2 porous thin films by polyethylene glycol templating and chemistry of the process, J. Eur. Ceram. Soc. 25 (2005) 673–679.
[14] R.S. Sonawane, B.B. Kale, M.K. Dongare, Preparation and photo-catalytic activity of Fe-TiO_2 thin films prepared by sol–gel dip coating, Mater. Chem. Phys. 85 (2004) 52–57.
[15] F. Bosc, P. Lacroix-Desmazes, A. Ayral, TiO_2 anatase-based membranes with hierarchical porosity and photocatalytic properties, J. Colloid Interf. Sci. 304 (2006) 545–548.
[16] M.M. Yusuf, H. Imai, H. Hirashima, Preparation of mesoporous TiO_2 thin films by surfactant templating, J. Noncryst. Soilds 285 (2001) 90–95.
[17] W.J. Zhang, Y.Q. He, Q. Qi, Synthesize of porous TiO_2 thin film of photocatalyst by charged microemulsion templating, Mater. Chem. Phys. 93 (2005) 508–515.
[18] E. Stathatos, P. Lianos, C. Tsakiroglou, Highly efficient nanocrystalline titania films made from organic/inorganic nanocomposite gels, Micropor. Mesopor. Mater. 75 (2004) 255–260.
[19] K. Ikeda, H. Sakai, R. Baba, K. Hashimoto, A. Fujishima, Photocatalytic reactions involving radical chain reactions using microelectrodes, J. Phys. Chem. B 101 (1997) 2617–2620.

[20] Y. Li, G. Lu, S. Li, Photocatalytic hydrogen generation and decomposition of oxalic acid over platinized TiO_2, Appl. Catal. A 214 (2001) 179–185.
[21] N. Serpone, P. Maruthamuthu, P. Pichat, E. Pelizzetti, H. Hidaka, Exploiting the interparticle electron transfer process in the photocatalysed oxidation of phenol, 2-chlorophenol and pentachlorophenol: chemical evidence for electron and hole transfer between coupled semiconductors, J. Photochem. Photobiol. A 85 (1995) 247–255.
[22] L.M. Peter, D.J. Riley, E.J. Tull, K.G.U. Wijayantha, Photosensitization of nanocrystalline TiO_2 by self-assembled layers of CdS quantum dots, Chem. Commun. (2002) 1030–1031.
[23] X.Z. Li, F.B. Li, C.L. Yang, W.K. Ge, Photocatalytic activity of WO_x–TiO_2 under visible light irradiation, J. Photochem. Photobiol. A: Chem. 141 (2001) 209–217.
[24] M.I. Litter, Heterogeneous photocatalysis: Transition metal ions in photocatalytic systems, Appl. Catal. B 23 (1999) 89–114.
[25] T. Ihara, M. Miyoshi, Y. Iriyama, O. Matsumoto, S. Sugihara, Visible-light-active titanium oxide photocatalyst realized by an oxygen-deficient structure and by nitrogen doping, Appl. Catal. B Environ. 42 (2003) 403–409.
[26] F. Kiriakidou, D.I. Koudarides, X.E. Verykios, The effect of operational parameters and TiO_2-doping on the photocatalytic degradation of azo-dyes, Catal. Today 54 (1999) 119–130.
[27] H. Einaga, S. Futamura, T. Ibusuki, Complete oxidation of benzene in gas phase by platinized titania photocatalysts, Environ. Sci. Technol. 35 (2001) 1880–1884.
[28] N. Serpone, E. Pelizzetti (Eds.), Photocatalysis-Fundamentals and Applications, Wiley-Interscience, New York, NY, USA, 1989.
[29] S. Castillo, M. Moran-Pineda, V. Molina, R. Gomez, T. Lopez, Catalytic reduction of nitric oxide on Pt and Rh catalysts supported on alumina and titania synthesized by the sol–gel method, Appl. Catal. B Environ. 15 (1998) 203–209.
[30] N. Strataki, P. Lianos, Optimization of parameters for hydrogen production by photocatalytic alcohol reforming in the presence of Pt/TiO_2 nanocrystalline thin films, J. Adv. Oxidation Technol. 11 (2008) 111–115.
[31] C.C. Chang, C.K. Lin, C.C. Chan, C.S. Hsu, C.Y. Chen, Photocatalytic properties of nanocrystalline TiO_2 thin film with Ag additions, Thin Solid Films 494 (2006) 274–278.
[32] J. Matsuoka, R. Naruse, H. Nasu, K. Kamiya, Preparation of gold microcrystal-doped oxide optical coatings through adsorption of tetrachloroaurate ions on gel films, J. Noncryst. Soilds 218 (1997) 151–155.
[33] J. Papp, H.S. Shen, R. Kershaw, K. Dwight, A. Wold, Titanium(IV) oxide photocatalysts with palladium, Chem. Mater. 5 (1993) 284–288.
[34] S. Jin, F. Shiraishi, Photocatalytic activities enhanced for decompositions of organic compounds over metal-photodepositing titanium dioxide, Chem. Eng. J. 97 (2004) 203–211.
[35] J. Araña, J.M. Doña-Rodríguez, O.O. González Díaz, E. Tello Rendóna, J.A. Herrera Melián, G. Colón, J.A. Navíob, J. Pérez Peña, Gas-phase ethanol photocatalytic degradation study with TiO_2 doped with Fe, Pd and Cu, J. Mol. Catal. A 215 (2004) 153–160.
[36] C. Belver, M.J. López-Muñoz, J.M. Coronado, J. Soria, Palladium enhanced resistance to deactivation of titanium dioxide during the photocatalytic oxidation of toluene vapors, Appl. Catal. B 46 (2003) 497–509.
[37] M.P. Kapoor, Y. Ichihashi, K. Kuraoka, Y. Matsumura, Catalytic methanol decomposition over palladium deposited on thermally stable mesoporous titanium oxide, J. Mol. Catal. A Chem. 198 (2003) 303–308.
[38] C.P. Sibu, S. Rajesh Kumar, P. Mukundan, K.G.K. Warrier, Structural modifications and associated properties of lanthanum oxide doped sol–gel nanosized titanium oxide, Chem. Mater. 14 (2002) 2876–2881.